THE JOURNAL OF PHYSICAL CHEMISTRY B

Article

pubs.acs.org/JPCB

Atomistic Molecular Dynamics Simulations of CO_2 Diffusivity in H_2O for a Wide Range of Temperatures and Pressures

Othonas A. Moultos,[†] Ioannis N. Tsimpanogiannis,[†] Athanassios Z. Panagiotopoulos,[‡] and Ioannis G. Economou*,[†]

[†]Chemical Engineering Program, Texas A&M University at Qatar, P.O. Box 23874, Doha, Qatar

[‡]Department of Chemical and Biological Engineering, Princeton University, Princeton, New Jersey 08544, United States

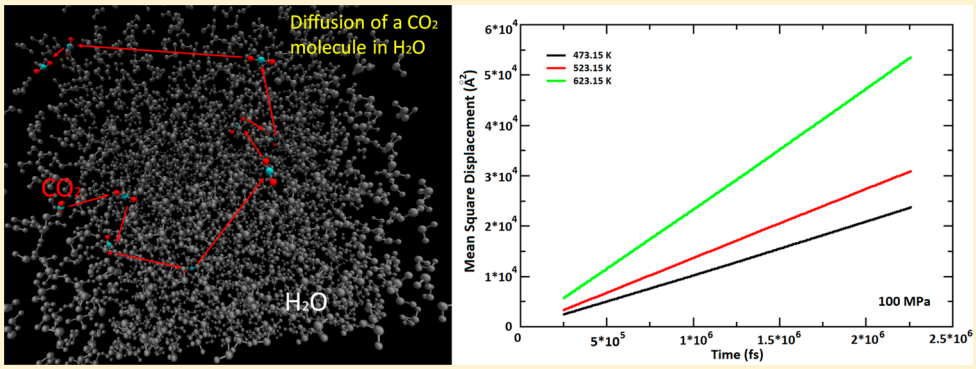

ABSTRACT: Molecular dynamics simulations were employed for the calculation of diffusion coefficients of CO_2 in H_2O. Various combinations of existing force fields for H_2O (SPC, SPC/E, and TIP4P/2005) and CO_2 (EPM2 and TraPPE) were tested over a wide range of temperatures (283.15 K < T < 623.15 K) and pressures (0.1 MPa < P < 100.0 MPa). All force-field combinations qualitatively reproduce the trends of the experimental data; however, two specific combinations were found to be more accurate. In particular, at atmospheric pressure, the TIP4P/2005−EPM2 combination was found to perform better for temperatures lower than 323.15 K, while the SPC/E−TraPPE combination was found to perform better at higher temperatures. The pressure dependence of the diffusion coefficient of CO_2 in H_2O at constant temperature is shown to be negligible at temperatures lower than 473.15 K, in good agreement with experiments. As temperature increases, the pressure effect becomes substantial. The phenomenon is driven primarily by the higher compressibility of liquid H_2O at near-critical conditions. Finally, a simple power-law-type phenomenological equation is proposed to correlate the simulation values; the proposed correlation should be useful for engineering calculations.

1. INTRODUCTION

Control of CO_2 concentration in the atmosphere is one of the greatest challenges that scientists and engineers face today worldwide. CO_2 is the most important of the so-called greenhouse gases, and there is a need for technologies for in situ capture and reliable storage.[1,2] CO_2 is typically captured from fossil fuel burning power plants, steel and iron manufacturing plants, cement, ammonia, and other chemical plants or other CO_2-intensive industries and transported to a storage site. The stream that is captured and transported contains a broad range of additional components, mostly in small concentrations (impurities), depending on the source. Typical impurities consist of other gases (such as N_2, O_2, H_2S, NO_x) and even H_2O. The CO_2 stream is stored in geological repositories, such as deep saline aquifers, coal beds, or hydrocarbon reservoirs.[3] In the latter case, CO_2 can be used to enhance oil recovery from a nondepleted well, a process known as tertiary oil recovery. For the efficient design of the entire carbon capture and sequestration (CCS) process and the safe depository of CO_2, accurate knowledge of primary and derivative thermodynamic (i.e., density, activity/fugacity coefficients, heat capacities, etc.), transport (i.e., viscosity, diffusion coefficients, etc.), interfacial, and phase equilibrium properties of the mixtures involved is necessary. The focus of this work is on the accurate calculation of the diffusion coefficient of CO_2 in H_2O for which some experimental data are available over a limited range of temperature and pressure conditions.[4−9]

The diffusion of dissolved gases in liquid solutions is encountered in many processes of industrial,[10] environmental,[11] geological,[12] and biological[13] interest. Therefore, understanding the detailed mechanism of diffusion of dissolved gases in liquids is an important component in the design, control, and optimization of the relevant complex processes. A number of experimental techniques have been reported and are discussed in detail by Cussler.[13] However, the experimental

Received: March 9, 2014
Revised: April 14, 2014
Published: April 21, 2014

   dx.doi.org/10.1021/jp502380r | J. Phys. Chem. B 2014, 118, 5532−5541

Table 1. Force-Field Parameters for H_2O and CO_2 Examined in This Study[a]

H_2O				CO_2		
	SPC	SPC/E	TIP4P/2005		EPM2	TraPPE
H−O−H (deg)	109.47	109.47	104.52	O−C−O (deg)	180	180
l_{O-H} (Å)	1.00	1.00	0.9572	l_{O-C} (Å)	1.149	1.16
σ_{O-O}	3.166	3.166	3.1589	σ_{C-C}	2.757	2.8
σ_{H-H}	0.00	0.00	0.00	σ_{O-O}	3.033	3.05
ε_{O-O}/k_B (K)	78.197	78.197	93.2	ε_{C-C}/k_B (K)	28.129	27.0
ε_{H-H}/k_B (K)	0.00	0.00	0.00	ε_{O-O}/k_B (K)	80.507	79.0
q_O (e)	−0.82	−0.8476	−1.1128	q_C (e)	0.6512	0.70
q_H (e)	0.41	0.4238	0.5564	q_O (e)	−0.3256	−0.35

[a]The parameters between unlike atoms are calculated by the combining rules of eqs 2 and 3.

determination of diffusion coefficients is often costly and difficult to perform, especially when measurements at high pressures and/or temperatures are needed. As a result, alternative approaches need to be considered. To this purpose, thermodynamic modeling at the continuum scale or atomistic simulations at the molecular scale provide reliable solution to extrapolate experimental data outside the range of measurements.

Mean-field-theory models for the diffusion coefficient have been proposed as semiempirical correlations based either on the kinetic theory of Chapman and Enskog[14] (i.e., Brokaw[15]) or on the hydrodynamic theory of Stokes and Einstein (i.e., Wilke and Chang[16]). Taylor and Krishna[17] provided an extensive discussion of the theory. In a recent study, Mutoru et al.[18] presented a detailed discussion of such models that are applicable to the binary CO_2-H_2O mixture. In addition, they presented an extended collection of experimental data and also reported a novel methodology for the calculation of the diffusion coefficient at infinite dilution of either of the two components.

Atomistic simulations, in particular using molecular dynamics (MD), can be a valuable tool to complement experimental measurements of transport properties. An advantage of the MD simulation method, compared to the macroscopic models, is that it can give insight into the systems at the molecular level. This approach has become more popular in recent years thanks to the significant increase of computing power, allowing for complex systems to be studied computationally for a time-span of many nanoseconds. A prerequisite for the successful implementation of MD simulations is the detailed and accurate description of the intra- and intermolecular interactions. For this reason, a large number of force fields, both for H_2O and CO_2, have been reported in the literature during the last decades. Detailed reviews of force fields for H_2O are presented by Vega et al.,[19,20] while for CO_2-related systems by Hamm et al.[12]

Molecular simulations of the phase equilibria of CO_2-H_2O mixtures have been reported by many researchers.[21−25] Despite the importance of the diffusivity of CO_2 in H_2O and the plethora of experimental data referring to it (see for example the detailed list of experimental data collected by Mutoru et al.[18]), molecular simulation studies of the diffusivity in the literature are few. More specifically, Lynden-Bell and co-workers[26] reported atomistic MD simulations for the prediction of CO_2 diffusivity in H_2O, using the GROMOS Lennard−Jones (LJ) parameters for CO_2 and retuned partial charges to match CO_2 quadrupole moment and the SPC/E model for H_2O. Their study aimed mostly in addressing the effects of the LJ size parameter (σ_{O-O}) and the partial charge size (quadrupole moment) on the D_{CO_2} at a single temperature of 293 K. Vlcek and co-workers[27] used the combination of the SPC/E−EPM2 models, in the temperature range of 298−348 K and pressure range of 0.1−40.5 MPa and focused on optimization of the force fields. Vlcek et al.[27] employed the coupling parameter scheme of the LJ unlike-pair interactions and succeeded in improving the predicted mutual solubility.[27] Additionally, Vlcek et al.[27] used the improved models in order to predict the mutual diffusivities. The reported results for the diffusion coefficient of CO_2 in H_2O are in good agreement with the experiments in the given temperature and pressure range and show no pressure effect (approximately 1% change from 1 to 40.5 MPa). Additional insights into the diffusion of CO_2 in H_2O have been given by Zeebe,[28] who presented results in the temperature range of 273−373 K, using the SCP/E model for H_2O and the model of ref 26 for CO_2. Zeebe[28] reported a fairly good agreement with the experimental values and showed a dependence of CO_2 diffusivity on the isotopic mass of the carbon atom. Finally, Garcia-Ratés et al.[29] reported values for the diffusivity of CO_2 in H_2O for a narrow range of temperatures and pressures; their study aimed at the determination of D_{CO_2} in brines.

From the above, it is clear that a comprehensive evaluation of various modern force-field combinations for H_2O and CO_2, with respect to their ability to predict the diffusivity D_{CO_2} over the range of temperatures and pressure that are relevant for CCS operations is lacking. This is the main focus of the current study. In particular, we report on an extensive series of MD simulations for a wide range of temperatures (298.15−623.15 K) and pressures (0.1−100.0 MPa), and for various combinations of force fields. We examine CO_2 in H_2O at a very low concentration, since the solubility of CO_2 in H_2O at the conditions of interest is generally small.

The structure of this paper is as follows. In Section 2, we present the intermolecular potentials and simulation methods that we used. In Section 3, we discuss our results, which generally are in good agreement with reported experimental data and clearly indicate that the diffusivity of CO_2 in H_2O increases with increasing temperature. The simulation results show that pressure has a marginal effect for temperatures up to 473.15 K, while for higher temperatures, the effect becomes substantial. The first part of the study focuses in the temperature range of 298.15−348.15 K and low pressure in order to identify which combinations of force fields perform better. Once two sets of accurate force fields are identified, they are used subsequently for the calculation of the diffusion coefficient of CO_2 in H_2O at higher pressure and temperature, of practical interest for CCS processes.[1,3] Finally, the diffusivity

dx.doi.org/10.1021/jp502380r | J. Phys. Chem. B 2014, 118, 5532−5541

values from the MD simulations are correlated using a simple phenomenological equation that can be further used for practical engineering applications, where the use of molecular simulation becomes impractical due to high-computational requirements. We close with a brief summary of our findings and possible future research directions.

2. MODELS AND METHODS

2.1. Intermolecular Potentials. For the representation of H_2O molecules, we used the SPC,[30] SPC/E,[31] and TIP4P/2005[32] models, while for CO_2, we employed the EPM2[33] and TraPPE[34] models. The SPC and SPC/E are rigid three-site H_2O models in which a LJ sphere is fixed on the oxygen atom. The electrostatic contributions are implemented by a positive partial charge located on each hydrogen atom and a negative partial charge located on the oxygen atom. The TIP4P/2005 force field is a 4-site model, where the additional site corresponds to the position of the negative charge, located on the bisector of the H−O−H angle at 0.1546 Å from the O atom. The EPM2 and TraPPE are rigid linear three-site CO_2 models, with partial charges fixed on the axis of symmetry of each molecule. More specifically, a negative partial charge is located on the O atom and positive ones on the C atoms. Values for the potential parameters are listed in Table 1. H_2O and CO_2 are modeled as molecular species. It is known that CO_2 is a weak acid that dissociates in the aqueous environment. On the basis of experimental evidence,[35] this dissociation is relatively small and can be safely ignored. Such an approach has been used widely in prior molecular simulation studies and macroscopic models.[36−39]

For the study of the binary H_2O-CO_2 mixture, five different combinations of models were considered here: (i) SPC with EPM2, (ii) SPC/E with EPM2, (iii) SPC/E with TraPPE, (iv) TIP4P/2005 with EPM2, and (v) TIP4P/2005 with TraPPE. Initial calculations using the SPC model indicated poor performance, when compared to the experiments (presented in detail in Section 3), and thus, only one combination containing this force field was examined.

Interactions between molecules i and j, with a total number of m and n sites, respectively, were calculated by the summation of LJ repulsion and dispersion interactions with the Coulombic contributions:

$$u_{ij} = \sum_{a=1}^{m}\sum_{b=1}^{n}\left(4\varepsilon_{ij}^{ab}\left[\left(\frac{\sigma_{ij}^{ab}}{r_{ij}^{ab}}\right)^{12} - \left(\frac{\sigma_{ij}^{ab}}{r_{ij}^{ab}}\right)^{6}\right] + \frac{q_i^a q_j^b}{4\pi\varepsilon_0 r_{ij}^{ab}}\right) \quad (1)$$

where ε_{ij}^{ab} and σ_{ij}^{ab} are the LJ interaction parameters between site a in molecule i and site b in molecule j, respectively, r_{ij}^{ab} is the distance between sites a and b, q_i^a and q_j^b are the charges on sites a and b, and ε_0 is the dielectric constant of the vacuum.

The LJ parameters for the interaction between atoms belonging to different molecules were calculated using the Lorenz−Berthelot combining rules.[40] An exception was made for the EPM2 model, for which the distance σ_{ij}^{ab} between unlike sites of CO_2 molecules was given by the geometric mean, in accordance with the original work.[33] Consequently, cross-interaction parameters were calculated from the expressions:

$$\varepsilon_{ij}^{ab} = (\varepsilon_i^a \varepsilon_j^b)^{1/2} \quad (2)$$

$$\sigma_{ij}^{ab} = \begin{cases} (\sigma_i^a \sigma_j^b)^{1/2} & \text{for } a, b = C_{CO2}, O_{CO2} \text{ for the EPM2 model} \\ \frac{1}{2}(\sigma_i^a + \sigma_j^b) & \text{otherwise} \end{cases} \quad (3)$$

2.2. Computational Details. MD simulations were performed in a cubic box, with periodic boundary conditions imposed in all directions, using the open-source large-scale atomic/molecular massively parallel simulator (LAMMPS).[41,42] For all simulations, the computational scheme was the following: initially, the system was allowed to equilibrate for a period from 1×10^6 to 2×10^6 time steps (corresponding to 1−2 ns) in the isothermal−isobaric (NPT) ensemble. This duration was more than sufficient for the system density to reach a constant value. The temperature and pressure were maintained constant using the Nosé−Hoover method,[43,44] with thermostat and barostat coupling constants equal to 200 and 1000 fs, respectively. Then, for each production run, a total of 5×10^6 time steps were performed in the microcanonical (NVE) ensemble. Monitoring the energy, temperature, and pressure during the production period showed that these properties were very well-stabilized, with small fluctuations present, which is typical for any MD simulation. In the Results and Discussion section, these stable values for temperature and pressure are reported. The integration time step, both for the equilibration period and the main simulation, was 1 fs. Calculations with a smaller time step equal to 0.5 fs, to ensure stability of simulations, resulted in essentially identical results, as shown in Figure 1. During the production period, the molecular trajectories were sampled every 5000 steps, resulting in a total of 1000 configurations per simulation, from which all properties of interest were calculated. The LAMMPS simulator provides a good degree of parallelization, and thus, each run was executed in 16 cores, of an Intel Xeon 2.7 GHz processor, and needed about 13−18 wall clock hours to be completed.

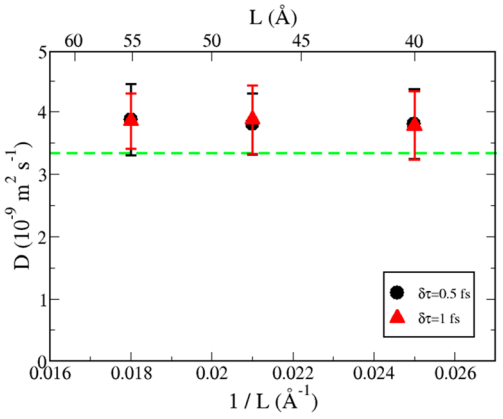

Figure 1. Diffusion coefficient of CO_2 in H_2O at 323.15 K and 0.1 MPa for various box sizes and two values of the integration time step for the MD simulations. The force fields used are SPC/E for H_2O and EPM2 for CO_2. The fit to experimental data by Versteeg et al.[4] is shown with the green dashed line.

The number of H_2O molecules in all simulations performed was equal to 2000, except for those cases presented in Figure 1, as discussed in the next paragraph. The number of CO_2 molecules was chosen such that the resulting CO_2 mole fraction was below the solubility of CO_2 for the particular

dx.doi.org/10.1021/jp502380r | J. Phys. Chem. B 2014, 118, 5532−5541

temperature and pressure conditions.[25,45] For most cases, up to 5 CO_2 molecules were used. This results in a mole fraction for CO_2 equal to 0.00249. Exceptions were made for the cases that the solubility was lower than this value (i.e., MD simulations at 0.1 MPa and various temperatures). The composition of the mixtures simulated here corresponds to close to infinite dilution limit; more than one CO_2 molecule was used in order to improve the statistics. In order to verify that results are independent of the number of CO_2 molecules in the low composition regime examined, the self-diffusion coefficient of CO_2 in 2000 H_2O molecules at 0.1 MPa and 323.15 K is shown in Figure 2 for the case of one, three, and five CO_2 molecules.

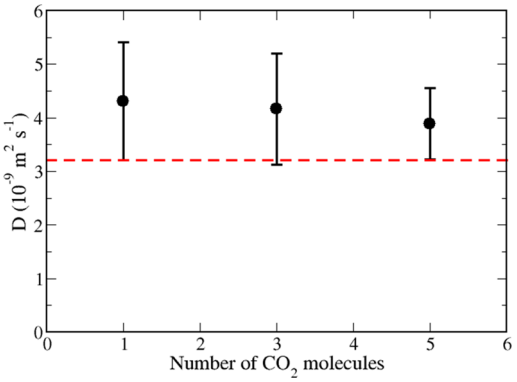

Figure 2. Diffusion coefficient of CO_2 in H_2O at 323.15 K and 0.1 MPa as a function of the number of CO_2 molecules. The force fields used are SPC/E for H_2O and EPM2 for CO_2. The red dashed line denotes the experimental value by Lu et al.[8]

The mean value is practically the same, but the statistical uncertainties decrease from 1.1 × 10^{-9} m^2 s^{-1} to 1.04 × 10^{-9} m^2 s^{-1} and finally to 0.67 × 10^{-9} m^2 s^{-1}.

A thorough investigation of system size effects was made by varying the number of H_2O molecules in the system. In Figure 1, we present simulation results for 5 EPM2 CO_2 molecules dissolved in 2000, 3500, and 5000 SPC/E H_2O molecules at 323.15 K and 0.1 MPa. The number of solvent molecules is proportional to the simulation box length, L, listed at the top axis. Although the self-diffusivity of CO_2 remains constant for the different box lengths, the computational time required for the simulation of the larger systems (i.e., 3500 and 5000 molecules) significantly increases (from approximately 20 ns/day to approximately 4 ns/day) and thus large systems are not computationally efficient. A similar analysis was performed for the calculation of a pure H_2O self-diffusion coefficient. The values for D_{H_2O} for the three systems, containing 2000, 3500, and 5000 H_2O molecules, were practically constant (4.3 ± 0.2, 4.2 ± 0.1, and 4.2 ± 0.1 × 10^{-9} m^2 s^{-1}, respectively), indicating that there are no system size effects present at this system size. Guevara-Carrion et al.[49] have shown that prediction of D_{H_2O} is not significantly affected once the size of the system exceeds 1500 H_2O molecules. On the basis of the observations from Figures 1 and 2, we chose to perform the MD simulations for the remainder of the study to systems that contain 2000 H_2O molecules and a time step of 1 fs.

Long-range Coulombic interactions were handled using the particle−particle particle−mesh (PPPM) solver,[46] a method very closely related to particle mesh Ewald but with a faster scaling.[47] The PPPM solver assumes conducting metal boundary conditions, while the relative quadratic mean error in per-atom forces was set equal to 10^{-4}. The cutoff distance

Table 2. Diffusion Coefficient of CO_2 in H_2O, for Various Combinations of Force Fields and Different Temperatures and Pressures[a]

		D_{CO_2} (10^{-9} m^2 s^{-1})				
T (K)	P (MPa)	SPC−EPM2	SPC/E−EPM2	SPC/E−TraPPE	TIP4P/2005−EPM2	TIP4P/2005−TraPPE
298.15	0.1	3.6 ± 0.8	2.7 ± 0.5	2.2 ± 0.5	2.0 ± 0.3	1.8 ± 0.4
323.15	0.1	5.5 ± 0.5	3.8 ± 0.6	3.9 ± 0.5	3.3 ± 0.5	3.2 ± 0.5
	20.0	–	3.9 ± 0.7	4.2 ± 0.8	3.9 ± 0.6	2.9 ± 0.5
	48.0	–	3.8 ± 0.5	3.9 ± 0.4	3.1 ± 0.6	2.9 ± 0.3
348.15	0.1	8.3 ± 0.6	5.9 ± 0.4	5.8 ± 0.7	4.4 ± 0.5	4.4 ± 0.4
	20.0	–	–	5.4 ± 0.9	4.4 ± 0.6	–
373.15	1.5	–	7.1 ± 0.7	6.9 ± 0.9	5.7 ± 0.6	5.7 ± 0.8
	20.0	–	6.4 ± 0.8	6.7 ± 0.8	5.7 ± 0.6	5.9 ± 0.9
	48.0	10 ± 1	6.5 ± 0.7	6.6 ± 0.8	6 ± 1	6.4 ± 0.8
398.15	20.0	–	–	9 ± 1	9 ± 1	–
423.15	20.0	–	–	12 ± 1	10 ± 1	–
448.15	20.0	–	–	14 ± 1	13 ± 1	–
473.15	20.0	–	–	16 ± 2	16 ± 2	–
	48.0	–	–	15 ± 2	15 ± 2	–
	100.0	–	–	14 ± 2	12 ± 1	–
523.15	20.0	–	–	24 ± 3	21 ± 2	–
	48.0	–	–	21 ± 3	18 ± 2	–
	100.0	–	–	18 ± 2	16 ± 1	–
573.15	48.0	–	–	28 ± 2	28 ± 3	–
623.15	20.0	–	–	55 ± 4	50 ± 4	–
	48.0	–	–	42 ± 3	35 ± 4	–
	100.0	–	–	32 ± 3	27 ± 4	–

[a]Statistical uncertainties are obtained as the standard deviation of 12 independent runs for each state point, as explained in the main text.

dx.doi.org/10.1021/jp502380r | J. Phys. Chem. B 2014, 118, 5532−5541

was set to 12 Å, both for the LJ interactions and the PPPM solver.

2.3. Mean Square Displacement and Statistical Uncertainties. All diffusion coefficient values presented here were calculated using Einstein's relation, according to which the diffusion coefficient is calculated from the mean square displacement:[48]

$$D = \lim_{t\to\infty} \frac{\langle [r_i(t) - r_i(0)]^2 \rangle}{6t} \quad (4)$$

where $r_i(t)$ is the unfolded position of the center of mass of CO_2 molecule i at time t, and the angle brackets indicate an ensemble average, over all solute molecules and all time origins. In order to improve the statistics of our results, the diffusion coefficient for each state point was calculated from 12 different simulations, each one starting from a completely different initial configuration and leading to a wide divergence of the trajectories of the molecules.

One should notice that although the calculation of the diffusion coefficient from the fit to the linear part of the mean square displacement is a straightforward, widely used methodology, it can yield significant uncertainties. It is well-known that the first part of the mean square displacement curve, corresponding to the collision-free motion of the solute, must be excluded from the calculations because of its nonlinear behavior.[40] Furthermore, for very long simulation times, poor statistics (relatively few samples) preclude an accurate calculation of the slope.

In the majority of the calculations, after the exclusion of both short-time and long-time segments, the time interval chosen for statistical analysis corresponded to 0.2−4.5 ns. For most of the cases examined, this time interval was further subdivided in two equal parts that were treated as independent simulations. This division was based on our observation that every solute molecule has passed 2 to 4 times through the simulation box boundaries during the simulation. The method described above ensured relatively low statistical errors, from 8 to 15%, that are similar or lower than the ones reported in other MD studies in the literature for the same mixture.[27,28] On the other hand, according to Mutoru et al.[18] who collected experimental diffusivities at atmospheric pressure, the available reported errors are lower than 10%. Additionally, for higher pressures Lu et al.[8] reported relative deviations up to 5%, while Cadogan et al.[9] reported experimental uncertainties that are equal to 0.023 D_{CO_2}.

3. RESULTS AND DISCUSSION

3.1. Temperature Dependence of Diffusivity and Accuracy of Various Force Fields. Initially, atomistic NVE MD simulations were performed at densities corresponding to a pressure of 0.1 MPa at temperatures of 298.15, 323.15, and 348.15 K. As mentioned in Section 2, the NVE MD simulations followed long NPT MD equilibration periods that resulted in stable energy and volume; the barostat and thermostat were turned off for the production period to prevent any effects on the mean-square-displacement dynamics. Results are shown in Table 2 and plotted in Figure 3. An important contribution of this work refers to MD simulation data at conditions beyond the range of temperature and pressure examined experimentally before. No data are available in the literature at 398.15 K and higher. The values presented in Table 2 will be useful in future development of theoretical models and for process design calculations.

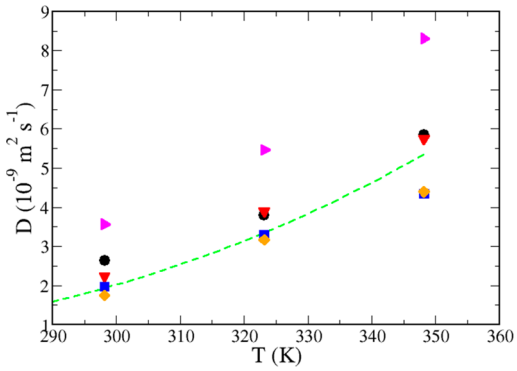

Figure 3. Diffusion coefficient of CO_2 in H_2O as a function of temperature at 0.1 MPa. Experimental data (dashed green line)[4] and MD simulation results: SPC-EPM2 (magenta ▷); SPC/E−EPM2 (black ●); SPC/E−TraPPE (red ▼); TIP4P/2005 (blue ■); and TIP4P/2005 (orange ◆). The statistical uncertainty of each state point is shown in Table 2 and is approximately 2−3 times the symbol size.

The diffusion coefficient increases with temperature, which is typical for gases dissolved in liquids.[4,13,17] Simulation results are compared to the data reported by Versteeg et al.,[4] who critically analyzed all experimental data available up to 1988, at 0.1 MPa and temperatures ranging from 273 to 348 K. From Figure 3, one can see that all combinations of force fields can qualitatively predict the behavior measured experimentally. However, there is substantial difference in the accuracy from different sets of calculations. Specifically, for the lower temperatures examined (298.15 and 323.15 K), simulations with TIP4P/2005 for H_2O perform better than the ones with the SPC/E and SPC models. The combination of TIP4P/2005 H_2O with EPM2 CO_2 shows almost perfect agreement (approximately 2% deviation) with experiments, while the combination of SPC with EPM2 overpredicts the diffusivity by approximately 90%. Predictions from the other force fields are in between the two extremes.

For the highest temperature shown in Figure 3 at 348.15 K, a different conclusion is drawn: calculations based on SPC/E H_2O show improved agreement with the experimental values, compared to the other models. In order to make the comparison clear, the absolute deviation between experimental data (Versteeg et al. correlation[4]) and MD predictions is presented in Figure 4, for the various combinations of force fields.

In order to obtain a better understanding of the accuracy of the H_2O force fields, we calculated the self-diffusion coefficient of H_2O in the same mixtures and results are presented in Table 3. There is a large number of studies[49−54] referring to pure H_2O self-diffusion coefficient, in the temperature range of 278−368 K and 0.1 MPa, so that an extensive evaluation of MD results can be made. In Figure 5a, the self-diffusion coefficient of H_2O as a function of temperature is shown. Both simulation results from this work and from the literature are shown. It can be seen clearly that new results are in very good agreement with the values by the other studies, indicating that the D_{H_2O} obtained from the mixture of H_2O with almost infinitely diluted CO_2 is very close to the D_{H_2O} calculated from MD simulations for pure H_2O. In Figure 5b, the self-diffusivity of H_2O along with the diffusivity of CO_2 in H_2O are presented.

dx.doi.org/10.1021/jp502380r | J. Phys. Chem. B 2014, 118, 5532−5541

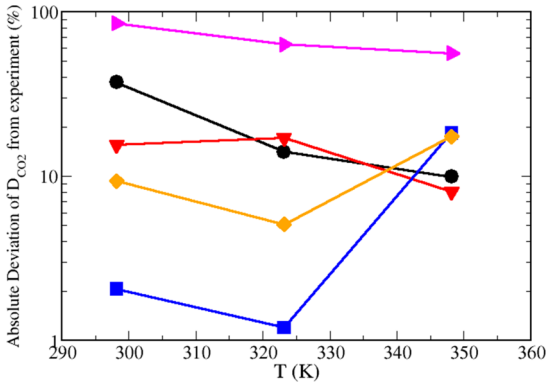

Figure 4. Absolute percentage deviation of the simulated diffusivity of CO_2 in H_2O from the experimental values of Versteeg et al.[4] at 0.1 MPa. All symbols are the same as in Figure 3 (lines are drawn to guide the eye).

Table 3. Self-Diffusion Coefficient of H_2O in its Mixture with Infinitely Diluted CO_2, for Various Force Fields, at the Temperature and Pressure Range Examined[a]

		D_{H_2O} (10^{-9} m^2 s^{-1})		
T (K)	P (MPa)	SPC	SPC/E	TIP4P/2005
298.15	0.1	3.6 ± 0.5	2.6 ± 0.1	2.1 ± 0.1
323.15	0.1	6.2 ± 0.5	4.3 ± 0.2	3.6 ± 0.1
	20.0	–	4.2 ± 0.1	3.6 ± 0.1
	48.0	–	4.2 ± 0.2	3.6 ± 0.1
348.15	0.1	8.8 ± 0.3	6.2 ± 0.2	5.4 ± 0.2
	20.0	–	6.2 ± 0.2	5.3 ± 0.1
373.15	1.5	–	8.4 ± 0.2	7.5 ± 0.1
	20.0	–	8.2 ± 0.1	7.4 ± 0.2
	48.0	10.7 ± 0.2	7.8 ± 0.3	7.4 ± 0.2
398.15	20.0	–	10.8 ± 0.3	9.7 ± 0.2
423.15	20.0	–	13.6 ± 0.5	12.6 ± 0.3
448.15	20.0	–	16.7 ± 0.5	15.4 ± 0.3
473.15	20.0	–	19.9 ± 0.4	18.7 ± 0.6
	48.0	–	19.4 ± 0.4	17.6 ± 0.5
	100.0	–	17.8 ± 0.3	17.0 ± 0.5
523.15	20.0	–	28.2 ± 0.8	25.9 ± 0.9
	48.0	–	26.4 ± 0.5	24.9 ± 0.8
	100.0	–	24.2 ± 0.7	22.7 ± 0.5
573.15	48.0	–	35.7 ± 0.8	32.3 ± 0.7
623.15	20.0	–	60 ± 2	51 ± 3
	48.0	–	48 ± 2	43 ± 1
	100.0	–	39.9 ± 0.8	38 ± 1

[a]Statistical uncertainties are obtained as the standard deviation of 12 independent runs for each state point, as explained in the main text.

The calculated values of D_{CO_2} and D_{H_2O} are very close to each other at 298.15 K, with a progressive deviation at higher temperatures. At 348.15 K, the difference is almost 25%. Consistently with Figure 5a, the SPC model overpredicts D_{H_2O} and the diffusivities predicted by SPC/E are always higher than the ones by TIP4P/2005.

3.2. Pressure Effect on Diffusivity. For the temperature range of 273.16−473.15 K and relatively high pressures up to approximately 49 MPa, experimental studies on CO_2 diffusivity in H_2O have been reported,[5−9,36] with those by Lu et al.[8] and Cadogan et al.[9] being the most comprehensive. In both cases, it was concluded that the effect of pressure is negligible, for the range of conditions examined. More specifically, Lu et al.[8]

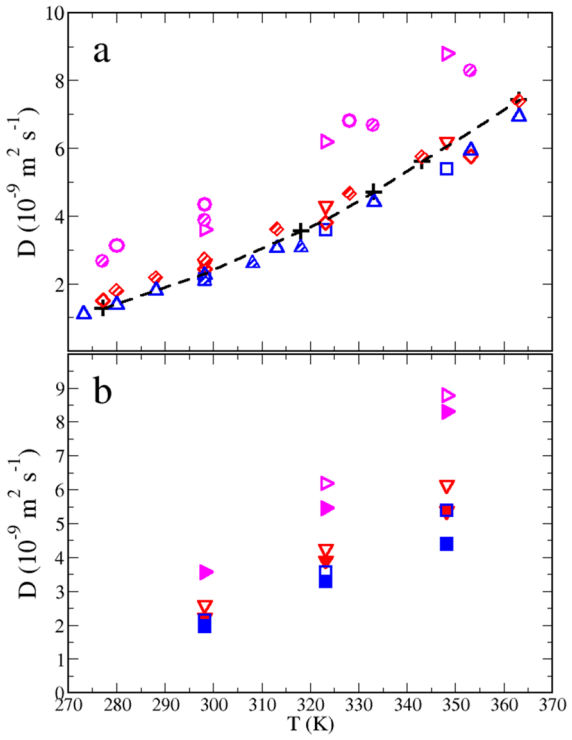

Figure 5. (a) Self-diffusion coefficient of pure H_2O and the (b) self-diffusion coefficient of pure H_2O and of infinitely diluted CO_2 in H_2O as a function of temperature at 0.1 MPa. Experimental data[51−54] (black +); SPC (magenta ▷); SPC/E (red ▽); TIP4P/2005 (blue □); SPC[49] (magenta ○); SPC[50] (magenta dashed circles); SPC/E[50] (red ◇); SPC/E[49] (red dashed diamonds); TIP4P/2005[49] (blue △); TIP4P/2005[19] (blue dashed triangles); and all other symbols are the same as in Figure 3. Errors bars are excluded for clarity. The dashed line, connecting the experimental values, is drawn to guide the eye.

reported a decrease in D_{CO_2} of less than 3% when the pressure increases from 30 to 45 MPa, at 393.15 K. Additionally, Cadogan et al.[9] reported differences in the diffusivity of CO_2 of around 1−2% for the pressure range of 14.0−48.6 MPa and temperatures ranging from 298 to 423 K.

In Figure 6, MD simulation results are shown for the diffusion coefficient of CO_2 in H_2O at 323.15 and 373.15 K, as a function of pressure, together with experimental data[8,9] for comparison. At each temperature, we performed simulations at three different pressures using various force fields. Calculations with SPC for H_2O were not performed at high pressures, due to the inaccuracy of the model at 0.1 MPa. Specifically, 0.1, 20.0, and 48.0 MPa were examined at 323.15 K, and 1.5, 20.0, and 48.0 MPa at 373.15 K. All simulations are in qualitative agreement with the experimental data and show a marginal pressure dependence on CO_2 diffusivity.

In Figure 6, one can see that at 323.15 K and 0.1 MPa, simulations with TIP4P/2005 are more accurate than the remaining ones. As the pressure rises, the same combinations seem to be in very good agreement with the experimental findings by Lu et al.,[8] with the combination of TIP4P/2005 with EPM2 to be the best performing one. However, the measurements reported by Cadogan et al.[9] are slightly higher, and agree more with the other combinations of models using SPC/E H_2O. For the highest pressure examined, at 48.0 MPa, the SPC/E−TraPPE combination is the most accurate, being in fairly good agreement with the experimental value of Cadogan

dx.doi.org/10.1021/jp502380r | J. Phys. Chem. B 2014, 118, 5532−5541

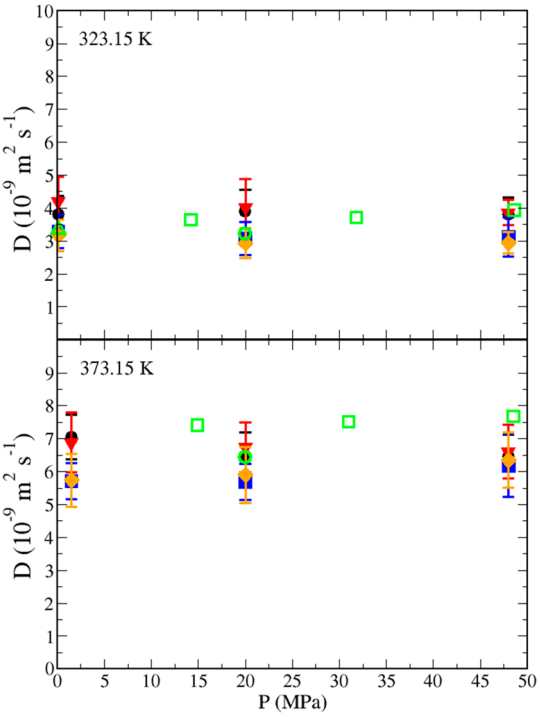

Figure 6. Diffusion coefficient of CO_2 in H_2O as a function of pressure at 323.15 K (top) and 373.15 K (bottom). Fit by Versteeg et al.[4] (green △); experimental data by Cadogan et al.[9] (green □); experimental value by Lu et al.[8] (green ○); and all other symbols are the same as in Figure 3.

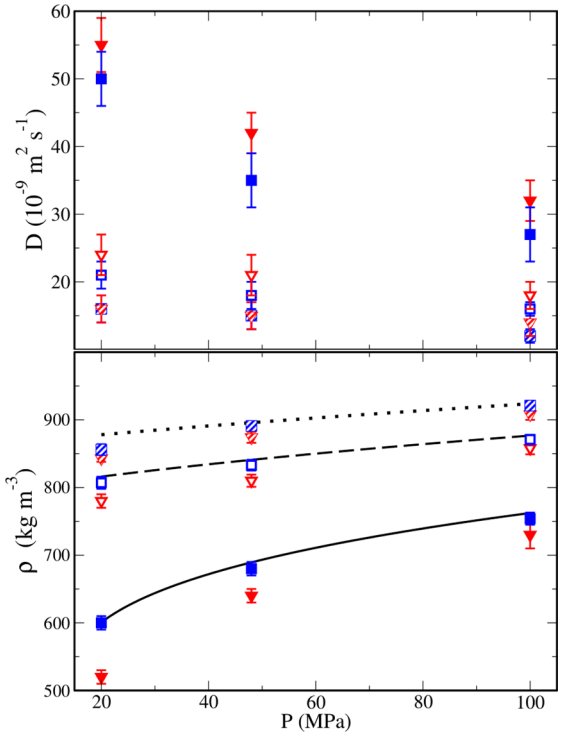

Figure 7. Simulated diffusion coefficients of CO_2 in H_2O (top) and densities (bottom) as a function of pressure for two force-field combinations: TraPPE-SPC/E (red triangles) and EPM2-TIP4P/2005 (blue squares) at 473.15 K (dashed symbols), 523.15 K (open symbols) and 623.15 K (solid color symbols). Black lines show experimental densities for pure H_2O (NIST database)[55] (473.15 K, dotted; 523.15 K, dashed; 623.15 K, solid).

et al.[9] ($D^{sim}_{CO_2}$ = 3.86 × 10^{-9} m^2 s^{-1} vs $D^{exp}_{CO_2}$ = 3.94 × 10^{-9} m^2 s^{-1}).

At 373.15 K, simulations seem to consistently underestimate the diffusion coefficient of CO_2 compared to experimental results of Cadogan et al.[9] However, the force field combinations that seem to perform better are the ones containing the SPC/E model for H_2O. For the intermediate pressure examined at 20.0 MPa, the combination of SPC/E with EPM2 is in almost perfect agreement with the experimental measurement by Lu et al.[8] ($D^{sim}_{CO_2}$ = 6.40 × 10^{-9} m^2 s^{-1} vs $D^{exp}_{CO_2}$ = 6.43 × 10^{-9} m^2 s^{-1}), while for the highest pressure of 48.0 MPa, the combination of SPC/E with TraPPE is closer to the experiments by Cadogan et al.[9] but still has a deviation from experimental data of around 20%.

At constant temperature well below the critical point, the density of a liquid solvent changes very little with pressure. As a result, the self-diffusion coefficient of the solvent or of a diluted solute, which is driven primarily by the free-volume of the system, remains unchanged. MD simulations of pure H_2O using the different force fields at 323.15 and 373.15 K and pressures from 0.1 to 48 MPa resulted in a density increase at constant temperature of 4%, which clearly justifies the marginal pressure effect on D_{CO_2}. The pressure effect on both density and self-diffusion coefficient becomes significantly more pronounced at higher temperatures, when the solvent becomes more compressible. MD simulations for D_{CO_2} in H_2O at 473.15, 523.15, and 623.15 K and different pressures are shown in Table 2 and Figure 7a. Simulations were performed only with the two best force-field sets (SPC/E−TraPPE and TIP4P/2005−EPM2), as evaluated in the lower temperature range. In addition, the density of the mixture at the same temperature and pressure values is shown in Figure 7b. Experimental data for the density of pure H_2O are also presented. It is clear that the pressure effect is now substantial, driven primarily by the relatively large change in solvent density. Figure 7b reveals that TIP4P/2005 is more accurate than TraPPE for the prediction of density for compressed liquid water.

More specifically, at 473.15 K, the density increase from 20 to 100 MPa K is 7.8% for SPC/E−TraPPE and 7.6% for TIP4P/2005−EPM2, while the decrease in D_{CO2} is 12.5% and 25%, respectively. At 523.15 K, the increase in density (from 20 to 100 MPa) and the decrease in D_{CO2} become larger for both sets of force fields. For SPC/E−TraPPE, the density increase is 10% and the D_{CO2} decrease is 25%, while for the TIP4P/2005−EPM2, the values are approximately 8% and 24%, respectively. Finally, at 623.15 K (approximately 20 K below H_2O critical temperature), the density increase for the first combination of models is approximately 40% and the decrease in diffusivity is 42%, while for the second combination, the respective values are 26% and 46%.

3.3. Phenomenological Model Development. An industrial application, where the accurate knowledge of the diffusion coefficient of CO_2 in H_2O is important refers to the CCS process,[1,3,18] which evolved in recent years as a viable solution for the control of CO_2 emissions in the atmosphere. For the design of a CCS process, engineering calculations are performed using physical property values at different conditions. It is impractical to use molecular simulations in this case; simpler but equally accurate correlations are needed.

As discussed in the previous section, recent experimental work[9] has concluded that for the binary CO_2-H_2O mixture, the

dx.doi.org/10.1021/jp502380r | J. Phys. Chem. B 2014, 118, 5532−5541

pressure has a very limited effect on the diffusion coefficient of CO_2 in H_2O for temperatures up to approximately 473.15 K. A similar conclusion was reached from our MD simulations. Therefore, in principle, one can construct a pressure-independent curve for the diffusion coefficient of CO_2 in H_2O, as a function of temperature.

In the current section, we use the two sets of force fields identified to perform better (i.e., SPC/E−TraPPE and TIP4P/2005−EPM2), in order to calculate the diffusion coefficient of CO_2 in H_2O for the temperature range of 348.15−473.15 K. Figure 8 shows the MD values for the diffusion coefficient of

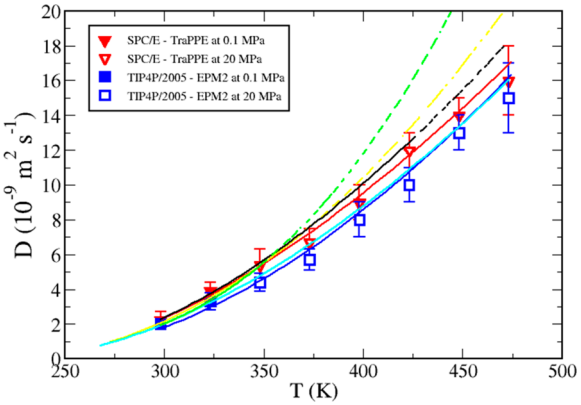

Figure 8. Diffusion coefficient of CO_2 in H_2O as a function of temperature from MD for two force-field combinations (points). Lines denote calculations from experimental correlations: Versteeg et al.[4] (green), Lu et al.[8] (cyan), and Cadogan et al.[9] (black) and MD correlations: Zeebe[28] (yellow), SPC/E−TraPPE from this study (red), and TIP4P/2005−EPM2 from this study (blue). Solid lines are within the range of development of the correlations, while dashed lines are extrapolations at higher temperatures.

CO_2 in H_2O, as a function of temperature, and for the two force-field combinations selected. The MD results are compared against the experimental values by Versteeg et al.,[4] by Lu et al.[8] and by Cadogan et al.[9] Lu et al.[8] used a power-law-type of equation to reproduce their experimental data expressed as follows:

$$D_{CO_2} = D_0\left(\frac{T}{T_s} - 1\right)^m \quad (5)$$

where D_o, T_s, and m are parameters adjusted to the data and are reported in Table 4. The same equation has been used by Zeebe[28] to reproduce his MD results (Figure 8). In the current study, we used a similar approach to correlate our MD results. In addition, the experimental data reported by Cadogan et al.,[9] were correlated here with the same expression. The corresponding fitted parameters are reported in Table 4. Our MD results are in good agreement with the experimental values. One should notice that the extrapolation of the correlation by Versteeg et al.,[4] at temperatures higher than 348.15 K, diverges significantly from the reported experimental data. On the other hand, the extrapolation of the correlation from Cadogan et al.'s data[9] remains in close proximity to the experimental data of Lu et al.[8]

4. CONCLUSIONS

In the present study, we have conducted MD simulations for the calculation of the diffusion coefficient of CO_2 in H_2O for a wide temperature (298.15−623.15 K) and pressure (0.1−100.0 MPa) range and for various combinations of existing force fields (SPC, SPC/E, and TIP4P/2005 for H_2O and EPM2 and TraPPE for CO_2).

Overall, MD results are in very good agreement with experimental data and indicate that the diffusivity of CO_2 increases with increasing temperature. The effect of pressure on D_{CO2} was shown to be marginal for temperatures lower than 473.15 K (consistent with the experimental data[8,9]), while it became significant for the higher temperatures examined (up to 623.15 K). Note that for the range of 473.15−623.15 K and pressures up to 100 MPa, the newly reported MD results are the only available in the literature. We found that for the case of constant pressure of 0.1 MPa and for low temperatures (below 323.15 K), the combination of models that result in more accurate predictions is the TIP4P/2005−EPM2. However, for temperatures above 323.15 K, the combination SPC/E−TraPPE performs better. Similar trends were observed for high pressures as well, with the two aforementioned combinations to be the more accurate ones.

The SPC force field which is the least accurate of the three models for pure H_2O properties from ambient temperature to near critical conditions results in poor predictions for the diffusion coefficient of CO_2. TIP4P/2005 is the most recent and most accurate force field for H_2O and, as a consequence, it provides overall the most accurate prediction for the diffusion coefficient of CO_2 for both CO_2 force fields. The effect of CO_2 force field on the accuracy of calculations seem to be of secondary importance. Clearly, the accurate representation of the solvent's density at a given temperature and pressure is the primary driver to succeed in the prediction of the solute diffusion coefficient. Consequently, although there are no experimental data to validate the argument, we believe that in the high temperature regime examined (473.15 K and above), TIP4P/2005 with either of the two CO_2 provides the most accurate prediction of the diffusion coefficient of CO_2.

Additional experimental work is needed at high temperature and pressure, in order to validate the calculations presented here. In addition, the force fields identified as the most accurate for the diffusivity coefficient prediction need to be validated for other transport properties (i.e., viscosity, surface tension, etc.). Ongoing work refers to simulations at the other end of the phase equilibrium envelope, that is the diluted H_2O diffusion coefficient in liquid and supercritical CO_2. Although hard to

Table 4. Parameters for the Diffusion Coefficient Expression (eq 5) for Various Sets of Experimental Data and MD Simulations

	T (K)	D_0 (10^{-9} m^2 s^{-1})	m	T_s (K)	R^2
experimental data: Lu et al.[8]	268.15−473.15	13.942	1.709	227.0	–
experimental data: Cadogan et al.[9]	298.15−423.15	15.922	1.690	227.0	0.998
MD: SPC/E−TraPPE (this work)	298.15−478.15	14.800	1.628	227.0	0.995
MD: TIP4P/2005−EPM2 (this work)	298.15−478.15	13.946	1.808	227.0	0.990
MD: Zeebe[28]	273.0−373.0	14.684	1.997	217.2	–

dx.doi.org/10.1021/jp502380r | J. Phys. Chem. B 2014, 118, 5532−5541

achieve, the ultimate goal of this work is to develop a multipurpose force field able to provide accurate prediction of phase equilibria, single phase thermodynamic, and transport properties of the H_2O-CO_2 mixture. Calculations with such a force field can be used to tune macroscopic engineering models, such as equations of state or empirical correlations, as the one shown in eq 5.

AUTHOR INFORMATION

Corresponding Author

*E-mail: ioannis.economou@qatar.tamu.edu.

Notes

The authors declare no competing financial interest.

ACKNOWLEDGMENTS

This publication was made possible by NPRP grant number 6-1157-2-471 from the Qatar National Research Fund (a member of Qatar Foundation). The statements made herein are solely the responsibility of the authors. We are grateful to the High Performance Computing Center of Texas A&M University at Qatar for generous resource allocation. We would like to thank S.P. Cadogan, G.C. Maitland, and J.P.M. Trusler for sharing their experimental data prior to publication.

REFERENCES

(1) Metz, B.; Davidson, O.; de Coninck, H.; Loos, M.; Meyer, L. *Carbon Dioxide Capture and Storage: Special Report of the Intergovernmental Panel on Climate Change*; Cambridge University Press: Cambridge, 2005.

(2) International Energy Agency. *A Policy Strategy for Carbon Capture and Storage*, IEA: Paris, 2012.

(3) Nordbotten, J. M.; Celia, M. A. *Geological Storage of CO_2: Modeling Approaches For Large-Scale Simulation*; John Wiley & Sons, Inc.: Hoboken, NJ, 2012.

(4) Versteeg, G. F.; Van Swaalj, W. Solubility and Diffusivity of Acid Gases (CO_2, N_2O) in Aqueous Alkanolamine Solutions. *J. Chem. Eng. Data* **1988**, *33*, 29−34.

(5) Frank, M. J. W.; Kuipers, J. A. M.; van Swaaij, W. P. M. Diffusion Coefficients and Viscosities of CO_2 + H_2O, CO_2 + CH_3OH, NH_3 + H_2O, and NH_3 + CH_3OH Liquid Mixtures. *J. Chem. Eng. Data* **1996**, *41*, 297−302.

(6) Hirai, S. O. K.; Yazawa, H.; Ito, H.; Tabe, Y.; Hijicata, K. Measurement of CO_2 Diffusion Coeffecient and Application of Lif in Pressurized Water. *Energy* **1997**, *22*, 363−367.

(7) Tewes, F.; Boury, F. Formation and Rheological Properties of the Supercritical CO_2−Water Pure Interface. *J. Phys. Chem. B* **2005**, *109*, 3990−3997.

(8) Lu, W.; Guo, H.; Chou, I. M.; Burruss, R. C.; Li, L. Determination of Diffusion Coefficients of Carbon Dioxide in Water Between 268 and 473 K in a High-Pressure Capillary Optical Cell with in Situ Raman Spectroscopic Measurements. *Geochim. Cosmochim. Acta* **2013**, *115*, 183−204.

(9) Cadogan, S. P.; Maitland, G. C.; Trusler, J. P. M. Diffusion Coefficients of CO_2 and N_2 in Water at Temperatures between 298.15 and 423.15 K at Pressures up to 45 MPa. *J. Chem. Eng. Data* **2014**, *59*, 519−525.

(10) Liu, X.; Martín-Calvo, A.; McGarrity, E.; Schnell, S. K.; Calero, S.; Simon, J.-M.; Bedeaux, D.; Kjelstrup, S.; Bardow, A.; Vlugt, T. J. H. Fick Diffusion Coefficients in Ternary Liquid Systems from Equilibrium Molecular Dynamics Simulations. *Ind. Eng. Chem. Res.* **2012**, *51*, 10247−10258.

(11) Bedient, P. B.; Rifai., H. S.; Newell, C. J. *Ground Water Contamination: Transport and Remediation*. Prentice-Hall: Englewood Cliffs: NJ, 1994.

(12) Hamm, L. M.; Bourg, I. C.; Wallace, A. F.; Rotenberg, B. Molecular Simulation of CO_2- and CO_3-Brine-Mineral Systems. *Rev. Mineral. Geochem.* **2012**, *77*, 189−228.

(13) Cussler, E. L. *Diffusion: Mass Transfer in Fluid Systems*, 3rd ed.; Cambridge University Press: Cambridge, 2009.

(14) Bird, R. B.; Klingenberg, D. J. Multicomponent Diffusion - A Brief Review. *Adv. Water Res.* **2013**, *62, Part B*, 238−242.

(15) Brokaw, R. S. Predicting Transport Properties of Dilute Gases. *Ind. Eng. Chem. Proc. Des. Dev.* **1969**, *8*, 240−253.

(16) Wilke, C. R.; Chang, P. Correlation of Diffrusion Coefficients in Dilute Solutions. *AIChE J.* **1955**, *1*, 264−270.

(17) Taylor, R.; Krishna, R. *Multicomponent Mass Transfer*; Wiley: New York, 1993.

(18) Mutoru, J. W.; Leahy-Dios, A.; Firoozabadi, A. Modeling Infinite Dilution and Fickian Diffusion Coefficients of Carbon Dioxide in Water. *AIChE J.* **2011**, *57*, 1617−1627.

(19) Vega, C.; Abascal, J. L. F.; Conde, M. M.; Aragones, J. L. What Ice Can Teach Us about Water Interactions: A Critical Comparison of the Performance of Different Water Models. *Faraday Discuss.* **2009**, *141*, 251−276.

(20) Vega, C.; Abascal, J. L. F. Simulating Water with Rigid Non-Polarizable Models: A General Perspective. *Phys. Chem. Chem. Phys.* **2011**, *13*, 19663−19688.

(21) Vorholz, J.; Harismiadis, V. I.; Rumpf, B.; Panagiotopoulos, A. Z.; Maurer, G. Vapor+Liquid Equilibrium of Water, Carbon Dioxide, and the Binary System, Water+Carbon Dioxide, from Molecular Simulation. *Fluid Phase Equilib.* **2000**, *170*, 203−234.

(22) Vorholz, J.; Harismiadis, V. I.; Panagiotopoulos, A. Z.; Rumpf, B.; Maurer, G. Molecular Simulation of the Solubility of Carbon Dioxide in Aqueous Solutions of Sodium Chloride. *Fluid Phase Equilib.* **2004**, *226*, 237−250.

(23) Lisal, M.; Smith, W. R.; Aim, K. Analysis of Henry's Constant for Carbon Dioxide in Water via Monte Carlo Simulation. *Fluid Phase Equilib.* **2005**, *228*, 345−356.

(24) Liu, Y.; Panagiotopoulos, A. Z.; Debenedetti, P. G. Monte Carlo Simulations of High-Pressure Phase Equilibria of CO_2−H_2O Mixtures. *J. Phys. Chem. B* **2011**, *115*, 6629−6635.

(25) Liu, Y.; Lafitte, T.; Panagiotopoulos, A. Z.; Debenedetti, P. G. Simulations of Vapor−Liquid Phase Equilibrium and Interfacial Tension in the CO_2−H_2O−NaCl System. *AIChE J.* **2013**, *59*, 3514−3522.

(26) In Het Panhuis, M.; Patterson, C. H.; Lynden-Bell, R. M. A Molecular Dynamics Study of Carbon Dioxide in Water: Diffusion, Structure and Thermodynamics. *Mol. Phys.* **1998**, *94*, 963−972.

(27) Vlcek, L.; Chialvo, A. A.; Cole, D. R. Optimized Unlike-Pair Interactions for Water-Carbon Dioxide Mixtures Described by the SPC/E and EPM2 Models. *J. Phys. Chem. B* **2011**, *115*, 8775−8784.

(28) Zeebe, R. E. On the Molecular Diffusion Coefficients of Dissolved CO_2, HCO^-_3, and CO_3^{2-} and their Dependence on Isotopic Mass. *Geochim. Cosmochim. Acta* **2011**, *75*, 2483−2498.

(29) Garcia-Ratés, M.; de Hemptinne, J.-C.; Avalos, J. B.; Nieto-Draghi, C. Molecular Modeling of Diffusion Coefficient and Ionic Conductivity of CO_2 in Aqueous Ionic Solutions. *J. Phys. Chem. B* **2012**, *116*, 2787−2800.

(30) Berendsen, H. J. C.; Postma, J. P. M.; van Gunsteren, W. F.; Hermans, J. Interaction Models for Water in Relation ot Protein Hydration. *Intermol. Forces* **1981**, 331−338.

(31) Berendsen, H. J. C.; Grigera, J. R.; Straatsma, T. P. The Missing Term in Effective Pair Potentials. *J. Phys. Chem.* **1987**, *91*, 6269−6271.

(32) Abascal, J. L. F.; Vega, C. A General Purpose Model for the Condensed Phases of Water: TIP4P/2005. *J. Chem. Phys.* **2005**, *123*, 234505−234512.

(33) Harris, J. G.; Yung, K. H. Carbon Dioxide's Liquid-Vapor Coexistence Curve and Critical Properties As Predicted by a Simple Molecular Model. *J. Phys. Chem.* **1995**, *99*, 12021−12024.

(34) Potoff, J. J.; Siepmann, J. I. Vapor-Liquid Equilibria of Mixtures Containing Alkanes, Carbon Dioxide, and Nitrogen. *AIChE J.* **2001**, *47*, 1676−1682.

(35) Zeebe, R. E.; Wolf-Gladrow, D. A. *CO_2 in Seawater: Equilibrium, Kinetics, Isotopes*; Elsevier: The Nederlands, 2001.
(36) Sell, A.; Fadaei, H.; Kim, M.; Sinton, D. Measurement of CO_2 Diffusivity for Carbon Sequestration: A Microfluid Approcach for Reservoir-Specific Analysis. *Environ. Sci. Technol.* **2013**, *47*, 71−78.
(37) Wollast, R.; Vanderborght, J. P. in *Chemistry of Aquatic Systems: Local and Global Perspectives*, Bidoglio, G.; Stumm, W., Eds.; Springer Science: Dordrecht, 1994; p 47.
(38) Espinoza, D. N.; Santamarina, J. C. Water-CO_2-Mineral Systems: Interfacial Tension, Contact Angle, and Diffusion: Implications to CO_2 Geological Storage. *Water Resources Research* **2010**, *46*, W07537 (1−10).
(39) Zeebe, R. E.; Wolf-Gladrow, D. A.; Jansen, H. On the Time Required to Establish Chemical and Isotopic Equilibrium in the Carbon Dioxide System in Seawater. *Mar. Chem.* **1999**, *65*, 135−153.
(40) Allen, M. P.; Tildesley, D. J. *Computer Simulation of Liquids*; Oxford University Press: New York, 1987.
(41) Plimpton, S. Fast Parallel Algorithms for Short-Range Molecular Dynamics. *J. Comput. Phys.* **1995**, *117*, 1−19.
(42) LAMMPS Molecular Dynamics Simulator. http://lammps.sandia.gov, accessed May 14, 2014.
(43) Nosé, S. A Molecular Dynamics Method for Simulations in the Canonical Ensemble. *Mol. Phys.* **1984**, *52*, 255−268.
(44) Hoover, W. G. Canonical Dynamics: Equilibrium Phase-Space Distributions. *Phys. Rev. A* **1985**, *31*, 1695−1697.
(45) Diamantonis, N. I.; Economou, I. G. Modeling the Phase Equilibria of a H_2O−CO_2 Mixture with PC-SAFT and tPC-PSAFT Equations of State. *Mol. Phys.* **2012**, *110*, 1205−1212.
(46) Hockney, R. W.; Eastwood, J. W. *Computer Simulation Using Particles*. Adam Hilger: NY, 1989.
(47) Pollock, E. L.; Glosli, J. Comments on P^3M, FMM, and the Ewald Method for Large Periodic Coulombic Systems. *Comput. Phys. Commun.* **1996**, *95*, 93−110.
(48) Einstein, A. On the Movement of Small Particles Suspended in Stationary Liquids Required by the Molecular-Kinetic Theory of Heat. *Ann. Phys.* **1905**, *17*, 549−560 in German.
(49) Guevara-Carrion, G.; Vrabec, J.; Hasse, H. Prediction of Self-Diffusion Coefficient and Shear Viscosity of Water and its Binary Mixtures with Methanol and Ethanol by Molecular Simulation. *J. Chem. Phys.* **2011**, *134*, 074508-1−074508-14.
(50) Raabe, G.; Sadus, R. J. Molecular Dynamics Simulation of the Effect of Bond Flexibility on the Transport Properties of Water. *J. Chem. Phys.* **2012**, *137*, 104512-1−104512-8.
(51) Krynicki, K.; Green, C. D.; Sawyer, D. W. Pressure and Temperature Dependence of Self-Diffusion in Water. *Farad. Discus. Chem. Soc.* **1978**, *66*, 199−208.
(52) Harris, K. R.; Woolf, L. A. Pressure and Temperature Dependence of the Self-Diffusion Coefficient of Water and Oxygen-18 Water. *J. Chem. Soc., Faraday Trans. 1: Phys. Chem. Cond. Phase* **1980**, *76*, 377−385.
(53) Yoshida, K.; Wakai, C.; Matubayasi, N.; Nakahara, M. A New High-Temperature Multinuclear-Magnetic-Resonance Probe and the Self-Diffusion of Light and Heavy Water in Sub- and Supercritical Conditions. *J. Chem. Phys.* **2005**, *123*, 164506-1−164506-10.
(54) Woolf, L. A. Tracer Diffusion of Tritiated Water (THO) in Ordinary Water (H_2O) under Pressure. *J. Chem. Soc., Faraday Trans. 1* **1975**, *71*, 784−796.
(55) Lemmon, E. W.; McLinden, M. O.; Friend, D. G. Thermophysical Properties of Fluid Systems. In *NIST Chemistry WebBook*, NIST Standard Reference Database Number 69, Linstrom, P. J., Mallard, W. G., Eds.; National Institute of Standards and Technology: Gaithersburg, MD, http://webbook.nist.gov (retrieved January 5, 2014).

■ NOTE ADDED AFTER ASAP PUBLICATION

This manuscript published ASAP on May 1, 2014. The Acknowledgment section was modified and the revised version reposted on May 5, 2014.